# Proton-Induced fluorescent switching of a dye containing imidazole and triphenylamine groups

HAI-GUANG ZHANG[a,b*], XU-TANG TAO[b], CUI-HUA DONG[a], JING-WEN XUE[a], ZHE WANG[a]
[a]*Key Laboratory of Pulp & Paper Science and Technology, Shandong Polytechnic University, Jinan, Shandong, China, 250353*
[b]*State Key Laboratory of Crystal Materials, Shandong University, Jinan, Shandong, China, 250100*

A new acid-base fluorescent switch: 2-((4'-di(4-methylphenyl)-aminophenyl)imidazo[4,5-f][1,10]-phenanthroline has been synthesized. The UV-Vis absorption and fluorescence emission spectra of it as well as its one derivative can be reversibly changed through protonation/deprotonation of imidazole and amine moiety by controlling the intramolecular charge transfer (ICT) process, leading to off-on-off fluorescent molecular switching. Their two-photon absorption (TPA) cross-sections were obtained as 310 and 392 GM in DMSO respectively. Meanwhile, Charge-transfer (CT) states of both compounds were calculated through theory methods to explain their acid-base-sensitive fluorescent properties.

(Received November 19, 2012; accepted April 11, 2013)

*Keywords*: Fluorescence switch, Triphenylamine, Intramolecular charge transfer (ICT), Two-photon absorption cross-section; synthesis

## 1. Introduction

The design and synthesis of fluorescent molecules exhibiting a switch function is an active area that has been intensively studied, which promises tremendous potential applications in the field of sensor fabrication [1-3]. Special attention has been given to the fluorescent molecules whose emission properties can be modulated through varying PH in solutions [4-9]. Aromatic amines are typical examples of pH fluorescent switches due to their reversible changes in fluorescent spectra induced by protonation/deprotonation [10-12]. Specifically, the amine is a strong donor while becomes a strong acceptor after being bound by a proton. As a result, the push–pull effect of intramolecular charge transfer (ICT) transition can be modulated, leading to a fluorescent molecular switch converting between two distinguished "on" and "off" states. On the other hand, imidazo[4,5-f][1,10]phenanthroline (abbreviated as IP) derivatives have shown interesting proton induced on-off emission switching characteristics [13-18]. In the previous literatures, one compound which connects TPA and IP moieties together: 2-(4'-tripenylamino)imidazo[4,5-f][1,10]phenanthroline (L2) have been reported for its ruthenium (□) and europium complexes were demonstrated as excellent fluorescent materials in organic light-emitting device (OLED) [19, 20]. But synthesis as well as understanding the photophysical properties and functions of new derivatives of L2 is still crucial for its exploration and applications.

In this work, one new compound: 2-((4'-di(4-methylphenyl)-aminophenyl)imidazo [4,5-f][1,10]-phenanthroline (L1) as well as L2 were synthesized (Scheme 1), The solvatochromic and solvatofluorchromic characteristics of both compounds have been investigated by means of qualitative spectroscopic analysis, by which an intramolecular charge transfer (ICT) can be identified. Particularly, it has been demonstrated that the UV-Vis absorption and fluorescent emission intensity of the two compounds can be reversibly changed via protonation/deprotonation of the imidazole and amine moiety by controlling ICT, leading to a off-on-off fluorescent molecular switch. Beside, the two-photon absorption (TPA) cross section and two-photon fluorescence emission of the two compounds are investigated, and the results are also presented in this paper. The charge-transfer (CT) states of the compounds were calculated using theory methods.

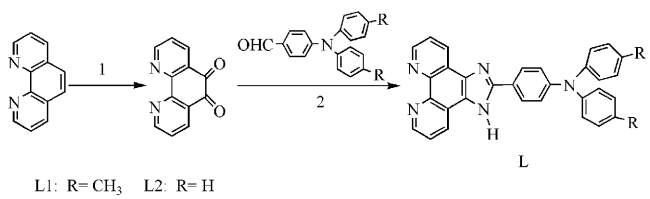


*Scheme 1. The synthesis and chemical structure of L1 and 2. 1. $H_2SO_4/HNO_3/KBr$ reflux 2h yield: 95 % 2.$NH_4Ac/CH_3COOH$ reflux 3h yield: 60 - 65 %*

## 2. Experimental

### 2.1 Instrument and physical measurements

Nuclear magnetic resonance spectra were recorded on Bruker A vance 300 MHz using DMSO-$d_6$ as solvent and $Me_4Si$ as internal reference. The electrospray mass spectrum (ES-MS) was determined on an ABI 4000 mass spectrograph. The diluted solution was electrosprayed with a needle voltage of +5.5Kv. The mobile phase was an aqueous solution of methanol (V/V, 1:1). Elemental analysis was performed using Vario. ELIII (German) elemental analyzer. The UV-Vis absorption spectra were recorded on a TU-1800 SPC spectrophotometer. The fluorescence emission spectra were obtained on an Edinburgh FLS920 spectrofluorometer equipped with a 450W Xe lamp and a time-correlated single-photon counting card. The fluorescence lifetime measurement was performed on the same spectrofluorometer with a hydrogen flash lamp (pulse duration<1 ns) as the excitation source. Re-convolution fits of the decay profiles were made with F900 analysis software to obtain the lifetime values.

The fluorescence quantum yields Φs were determined by the literature method using coumarin 307 as standard (ethanol, $\Phi = 0.56$), which has the same concentration with the samples as reference [21]. Two-photon excited fluorescence (TPEF) spectra were noted on an OOIBASE32 spectrophotometer. The pump laser beam came from a mode-locked Ti:sapphire laser system, pulse duration 200 fs, repetition rate of 76 MHz (Coherent Mira900-D). All measurements were carried out in air at room temperature. TPA cross-sections were measured using two-photon-induced fluorescence measurement technique [22].

### 2.2 Chemicals and synthesis

The compound 1, 10-phenanthroline-5, 6-dione [23] was synthesized according to a method in the literature with a high yield of 95%. The other reagents were obtained commercially and used as supplied. 2-((4'-di(4-methylphenyl)amino-phenyl)imidazo [4,5-f][1,10]phenanthroline (L1) was prepared according to the procedures in the literature [19, 20] (see Scheme 1).

L1: A mixture of 1,10-phenanthroline-5,6-dione(5 mmol), ammonium acetate (100 mmol), aldehyde (6 mmol) and glacial acetic acid (60 mL) was refluxed for about 2 h, then cooled to room temperature. The yellow precipitate was collected and washed with hot water after the reaction solution being neutralized with concentrated aqueous ammonia. The crude product was purifies by recrystallization from ethanol to obtain L1 as yellow needle crystals (yield: 62%). $^1$H NMR (DMSO-$d_6$, 300 MHz), δ (ppm): 13.57 (s, 1H) , 9.02 (d, 2H), 8.91 (d, 2H), 8.12 (d, 2H), 7.82 (m, 2H), 7.18 (d, 4H), 7.04 (m, 6H), 2.30 (s, 6H). $^{13}$C NMR (DMSO-$d_6$, 300 MHz), δ (ppm): 151.27, 149.37, 148.15, 144.62, 143.75, 136.22, 133.65, 130.72, 130.05, 127.84, 126.57, 125.57, 123.81, 122.81, 119.73, 20.91. ES-MS, $C_{33}H_{25}N_5$ ($M^+$+H) m/z (%): Calcd: 492.6, Found: 492.6 (100%). Element analysis: $C_{33}H_{25}N_5{\cdot}CH_3CH_2OH$ Calcd: C, 78.18; H, 5.81; N, 13.03% Found: C, 77.45; H, 5.42; N, 13.53%.

L2 was prepared using the same procedure as that of L1 and obtained as yellow crystal solid (yield: 65%). The $^1$H NMR spectra of L2 was the same as that reported in the literature. $^1$H NMR ($d_6$-DMSO, 300 Hz) δ(ppm): 9.03 (d, 2H), 8.92 (d, 2H), 8.16 (d, 2H), 7.84 (m, 2H), 7.40 (m, 4H), 7.15 (m, 8H).

## 3. Results and discussion

### 3.1 UV-Vis absorption and fluorescence emission spectra of L1 and 2

The UV-Vis absorption and fluorescence emission spectra in different solvents for L1 and 2 are depicted in Fig. 1 and 2 respectively. They were all measured at a concentration of $c = 1 \times 10^{-5}$ mol/l. As shown in Fig. 1, all absorption spectra showed two major absorption bands with their maxima peak located at 290 and 360 nm respectively. The absorption spectra of two compounds were all blue-shifted as the solvent polarity increased, exhibiting typical ICT characteristics (Table 1).

*Table 1 Photophysical properties of L1 and 2.*

| Compds | Solvent | $\lambda_{max}^{abs}$ /nm | $\lambda_{max}^{em}$ /nm | $\Phi_F$ | τ/ns |
|---|---|---|---|---|---|
| L1 | toluene | 283,358 | 452 | 0.53 | 1.96 |
| | $CH_2Cl_2$ | 286,360 | 482 | 0.50 | 1.80 |
| | ethyl | 285, 362 | 462 | 0.47 | 1.63 |
| | DMF | 291,366 | 498 | 0.39 | 1.48 |
| | DMSO | 292,366 | 506 | 0.36 | 1.25 |
| L2 | toluene | 287,357 | 440 | 0.62 | 2.08 |
| | $CH_2Cl_2$ | 288,360 | 468 | 0.55 | 1.94 |
| | ethyl | 285,359 | 449 | 0.54 | 1.84 |
| | DMF | 289,360 | 487 | 0.46 | 1.56 |
| | DMSO | 292,362 | 496 | 0.38 | 1.44 |

$\lambda_{max}^{abs}$ and $\lambda_{max}^{em}$ are UV-Vis absorption and fluorescence maxima peak, respectively. $\Phi_F$ is fluorescence quantum yield determined using coumarin 307 as the standard. τ is fluorescence lifetime.

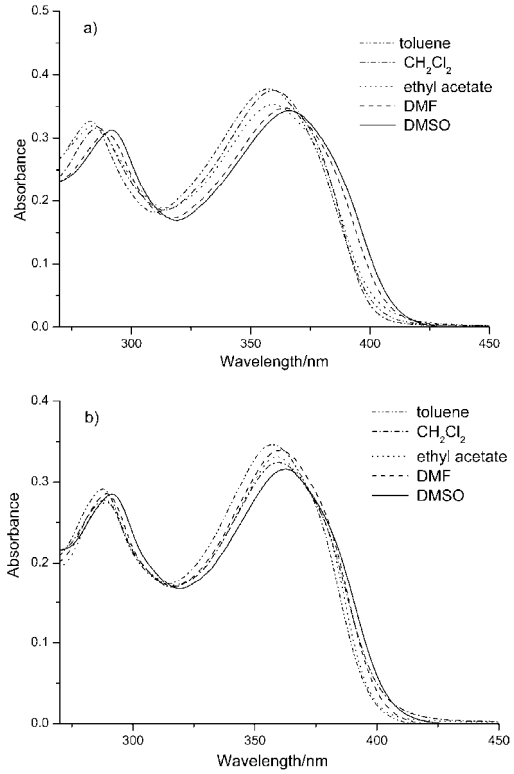


*Fig. 1. UV-Vis absorption spectra of L1 and 2 in different solvents (c = 1 × 10$^{-5}$ mol/l). (a): L1, (b): L2.*

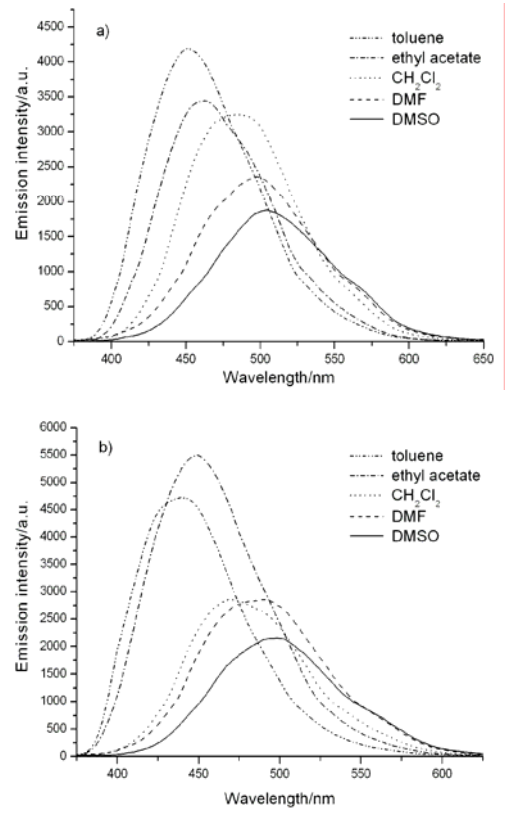


*Fig. 2. The emission spectra of L1 and 2 in different solvents (c = 1 × 10$^{-5}$ mol/l). (a): L1 (excited by 366 nm), (b): L2 (excited by 362 nm).*

As shown in Fig. 2, both L1 and 2 exhibited strong fluorescence emission with their maximum emission wavelengths ( $\lambda_{\max}^{em}$ ) located at range from 452 to 506 nm (L1) and from 440 to 496 nm (L2), respectively. For both L1 and 2, as the solvent polarity increased, the $\lambda_{\max}^{em}$ increased while emission intensities decreased. This can be explained by the fact that the excited state of the target compound may possess higher polarity than that of the ground state, for the solvatochromism is associated with the energy level lowering. Increased dipole-dipole interaction between the solute and solvent leads to lowering the energy level greatly [24, 25]. In addition, the excited state rapidly undergoes nonradiative transition to triplets, which results in a marked decrease in Φ and τ with increasing solvent polarity (Table 1).

### 3.2 Reversible absorption changes during deprotonation and protonation

The variations in UV-Vis absorption spectra of both compounds responding to acid-base were measured in DMSO/$H_2O$ ($V_{DMSO}/V_{H2O}$ = 9:1) with a concentration of c = 5 × $10^{-5}$ mol/l. The titration experiments were conducte d using Gilson P20 Pipetman microburettes in which 0.1 mol/l HCl or 0.1 mol/l NaOH aqueous solution was employed.

As shown in Fig. 3, during NaOH aqua titration to the neutral solutions, the absorptions of L1 at 292 nm (292 nm for L2) progressively decreased until the absorption almost completely disappeared, simultaneously, a new absorption band around 311 nm (313 nm for L2) gradually formed and developed. Particularly, the presence of an isosbestic points at 299 nm (310 nm for L2) indicates that only two species coexisted at the equilibrium. Meanwhile, the absorption band at 366 nm (362 nm for L2) was strengthened and blue-shifted 5 nm (2 nm for L2). In addition, during the NaOH titration, the colors of the solutions of both compounds gradually changed from colorless to greenish blue due to the deprotonation of IP moiety. However, the color as well as the absorption spectra can be recovered after adding appropriate amount of HCl, indicating the occurrence of reversible reactions. On the other hand, during the titration of the neutral solutions with the HCl solution, no appreciable changes in absorption spectra were observed until 20 times mole amount of HCl relative to the titrand has been added, indicating a negligible effect of protonation on the ground states of L1 and 2.

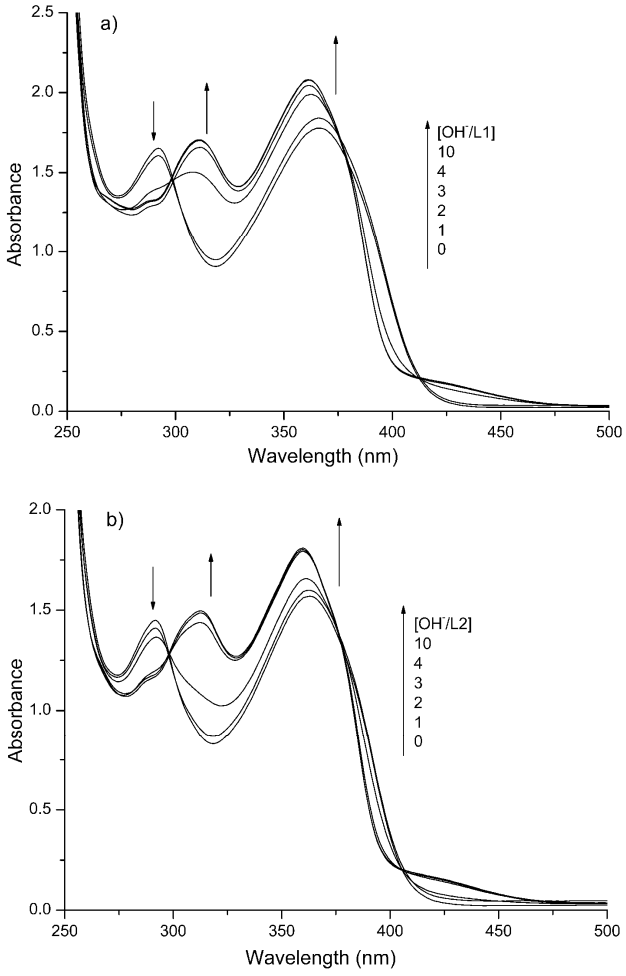


*Fig. 3. UV–Vis spectra of L1 and 2 during the titration of NaOH aqua (c = 5 × $10^{-5}$ mol/l). (a: L1, b: L2).*

### 3.3 Reversible fluorescent changes during deprotonation and protonation

The variations in fluorescence emission spectra of L1 and 2 responding to acid-base were measured in the same solutions as UV-Vis absorption measure. As shown in Fig. 4, L1 and 2 exhibited strong fluorescence emissions with their $\lambda_{max}^{em}$ located at 500 nm (L1, excitation at 366 nm) and 510 nm (L2, excitation at 362 nm) respectively. However, upon the addition of NaOH, their emissions decreased significantly while the $\lambda_{max}^{em}$ s were red-shifted. The emission spectra of both compounds no longer changed remarkably after more than 3 times mole amount NaOH were added, indicating almost complete deprotonation of imidazole. In Fig. 4(a) and (b), the fluorescent intensity of deprotonated L1 and 2 were only 1/5 and 1/3 of that of original L1 and 2 respectively, and their $\lambda_{max}^{em}$ s were red shifted about 36 and 33 nm respectively. It can be attributed to the quenching of fluorescence emissions caused by the photo-induced electron transfer (PET) from IP to phenylamine group that was induced by enhanced electron density in IP group as a result of the deprotonation of imidazolyl group. On the other hand, as Fig. 4(c) and (d) shown, the fluorescent emissions of L1 and 2 decreased accompanying the addition of HCl into the neutral solutions until their emissions have been completely quenched with $\lambda_{max}^{em}$ s do not shift. As the acid was added into the neutral solutions, we proposed that the proton can be rapidly bound onto the nitrogen atom of phenylamine rather than imidazole. It is because that the imidazole ring has weak basic property and the proton incorporation into the neutral imidazole only occurs in a pH range 1~3 [13-18], while the phenylamine moiety has strong basic property [10-12]. In addition, in the presence of proton, a positively charged benzene amino moiety in L1 and 2 was formed, then the electron density in the nitrogen of benzene amino group decrease significantly and the push–pull effect of ICT transition was reduced, which quenching the fluorescence emission. In the experiments, during HCl or NaOH solution was added into the above basic or acid solutions, the fluorescent emission gradually increased until the initial intensity was completely recovered, which means the change of fluorescent emissions induced by acid and base were reversible.

From above, we can conclude that the fluorescent emissions of L1 and 2 were the strongest in the neutral solutions because where the ICT from the donor amine moiety to the acceptor IP moiety can be mostly enhanced. Both compounds L1 and 2 can behave as off-on-off emission switches via deprotonation/protonation by adding base/acid.

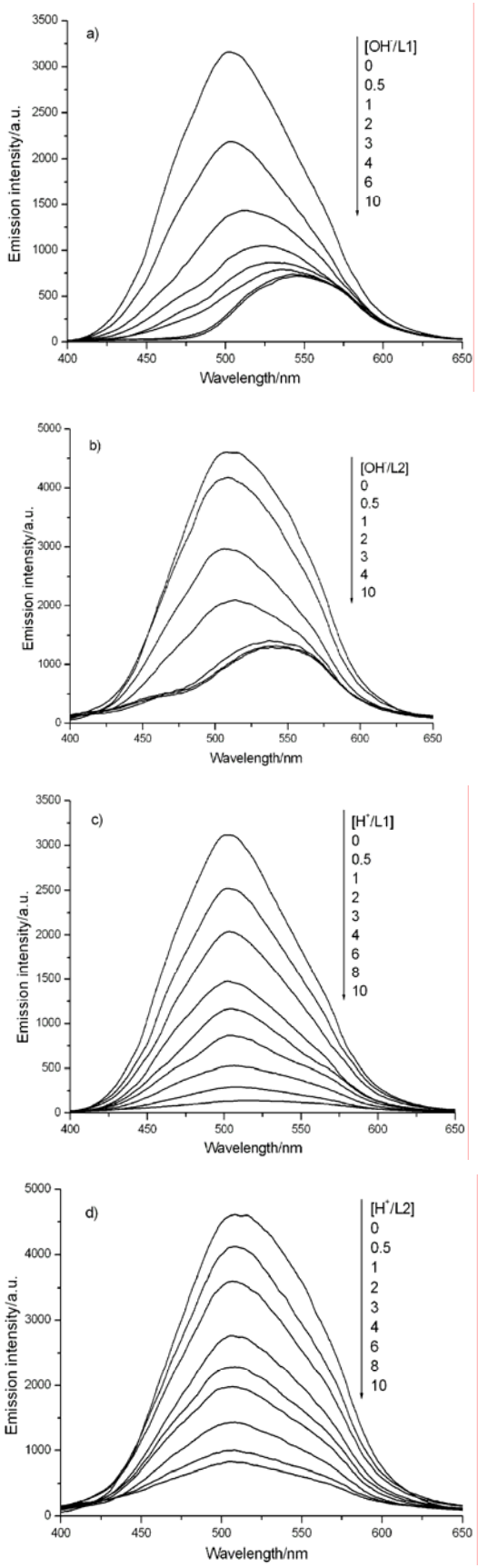


*Fig. 4. The emission fluorescent spectra of L1 and 2 during the titration of NaOH (c = 5 × $10^{-5}$ mol/l). (a: L1, b) L2 or HCl aqua c) L1 and d): L2.*

### 3.4 Two-photon excited fluorescence (TPEF) spectra and two-photon absorption (TPA) cross-section

Two-photon absorption (TPA) is the simultaneous absorption of two photons in order to excite a molecule from one state (usually the ground state) to a higher energy electronic state, and the fluorescent emission excited by TPA is usually called two-photon excited fluorescence (TPEF). Comparison with single-photon fluorescent sensors, two-photon fluorescent sensors excited in the near-infrared (NIR) region show very low background light, weak photodamage, highly transmission at the low incident intensity. These characters can make such two-photon chromophores suitably act as fluorescent labels in bioimage. Then investigation of two-photon properties of these two compounds was also carried out.

The two-photon excited fluorescence (TPEF) spectra of L1 and 2 were observed in DMSO with the concentration c = 1 × $10^{-3}$ mol/l. As shown in Fig. 5, excitated by 730 nm wavelength, both L1 and L2 emission two-photon fluorescence with their maxima peaks ($\lambda_{max}^{(2f)}$) located at 550 and 545 nm respectively. The two-photon absorption (TPA) cross-section $\sigma_s$ was calculated by using the two-photon-induced fluorescence measurement technique with the following equation[22]

$$\sigma_s = \sigma_r \frac{\Phi_r}{\Phi}\frac{c_r}{c}\frac{n_r}{n}\frac{F_s}{F_r}$$

where the subscripts s and r refer to the sample and the reference material, respectively. The terms *c* and *n* are the concentration and refractive index of the sample solution, respectively. Φ is the fluorescence quantum yield. *F* is two-photon excited fluorescence integral intensity. $\sigma_r$ is the TPA cross section of the reference molecule and fluorescein in water with pH 11 was selected as the standard [26]. The intensities of the TPEF spectra of the reference and the sample emitted at the same excitation wavelength were determined. By referencing the TPA cross-section of flouorescein to be 36 GM, the TPA cross section ($\sigma_s$) of L1 and 2 in DMSO solution were determined to be 310 and 392 GM, where 1 GM (GöppertMayer) = 1 × $10^{-50}$ $cm^4$ $photon^{-1}$ $molecule^{-1}$, Both $\sigma_s$ are medium in that of many compounds in the literatures.

Variations of TPEF spectra of L2 due to acid-base changes were investigated in mixed neutral solvent: DMSO/$H_2O$, acidic solvent: DMSO/0.1 mol/l HCl aqueous solution and basic solvent: DMSO/0.1 mol/l NaOH aqueous solution. The mixed ratio in three solvents was 9:1 (V/V). But the TPEF spectra of L1 was not measured in these three solutions because bad dissolubility

induced by the water. As Fig. 6 shown, the TPEF spectra changed in the same way as one-photon excited fluorescence (OPEF) as mentioned above. Compared in neutral solvents, a fluorescent emission weaken and $\lambda_{max}^{(2f)}$ red-shifted from 556 to 572 nm were observed in basic solvents and the $\sigma_s$ decreased from 239 to 106 GM. But in acidic solvent, the two-photon fluorescent emission was quenched seriously and $\lambda_{max}^{(2f)}$ is obscure, the $\sigma_s$ was calculated as 20 GM. From above, we can conclude that the ICT and PET process in L2 can also influence its TPEF in the same way as OPEF.

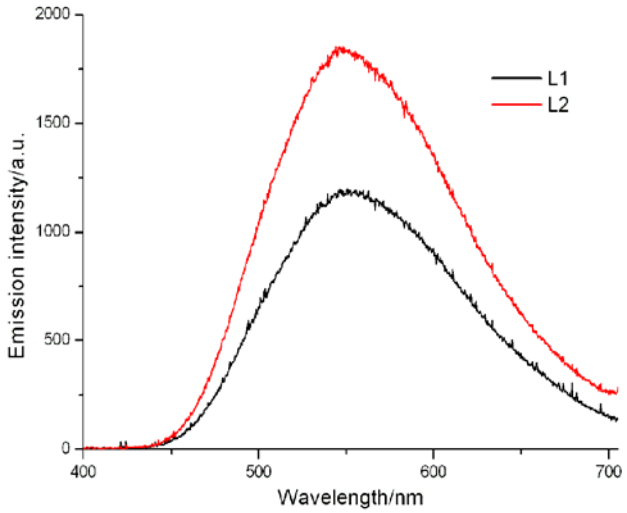


*Fig. 5. TPEF spectra of L1 and 2 in DMSO at a concentration of 1 × $10^{-3}$ mol/l (excited by 730 nm wavelength).*

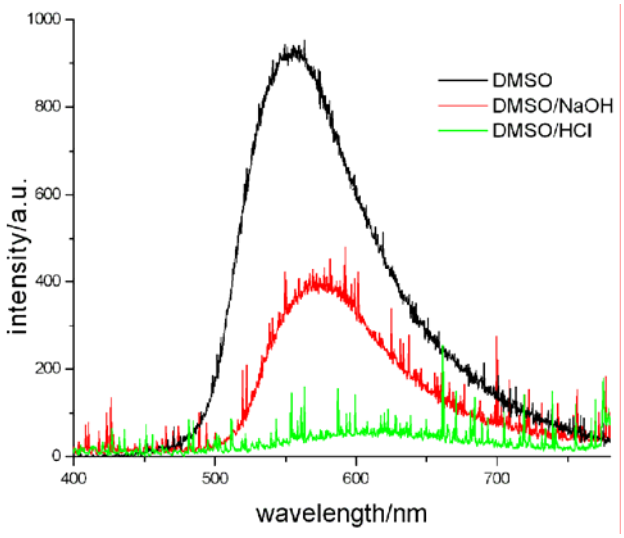


*Fig. 6. TPEF spectra of L2 in DMSO at a concentration of 1×$10^{-3}$ mol/l (with and without acid or base). (excited by 730 nm wavelength).*

As mentioned above, the OPEF and TPEF of these two compounds are sensitive to the acid-base in the solution and they act as off-on-off fluorescent molecular switching. In the other experiments, we have synthesized one compound: 2-{4-[(dicyanomethylidene-5,5-dimethylcyclohexl)vinyl]phenyl}imidazo[4,5-*f*][1,10]phenanthroline (DDVPIP), in which both imidazo[4,5- f][1,10]phenanthroline and dicyano moieties are electron accepted groups and it possess acceptor–π–acceptor (A–π–A) molecular structures [27]. On the contrary to L1 and 2, the OPEF and TPEF of DDVPIP are enhanced in the basic solution but weakened in acidic solution, and we supposed the electron withdrawal property of dicyano moiety in the molecular is crucial for this optical property. An ICT from deprotonated IP to dicyano moiety along with phenyl and three vinyl groups can be found in the deprotonated DDVPIP. Based on this fact, we can conclude that the electron donor or acceptor property of the moieties connected with IP group have oppositive influence on their acid-base-sensitive fluorescent property. The OPEF and TPEF of these compounds can be modulated through modulating the ICT process in the molecular.

### 3.5 Theoretical calculation of L1 and 2

To be able to gain a deeper insight into the ICT process of L1 and 2 compounds, the theoretical calculations have been conducted based on Gauss03 program in which the structures of both compounds were perfectly optimized at the B3LYP/6-31G(d) level. The electron distribution in HOMO and LUMO energy states of L1, L1OH (deprotonation) and L1H (protonation) are shown in Fig. 7. According the discussion above, we supposed the $H^+$ atom was connected with the N of phenylamine in the calculation of L1H (protonation). As shown in Fig. 7(a), the electron distribution in the frontier MOs of neutral L1 revealed a HOMO–LUMO excitation in which the electron distribution extended from TPA moiety to the IP moiety, exhibiting strong ICT migration characteristics. Meanwhile, the electron distribution in the frontier MOs of deprotonated L1, as shown in Fig. 7(b), revealed a HOMO–LUMO excitation in which the electron migrated from IP to TPA moiety, indicating the occurrence of an efficient PET process. It was well consistent with the PET quenching observed in the base solutions in the experiments. Similarly, an electron migration from the IP moiety to the phenyl ring of TPA moiety has been observed in protoned L1, as shown in Fig. 7(c) by the electron distribution in HOMO–LUMO excitation. However, the ICT migration from TPA to IP can not be found here, which is consistent with the observed fluorescent quenching in the acid solutions during the experiments. The similar calculations have also been conducted for L2, and the results showed that its deprotoned/protoned states exhibited the similar HOMO–LUMO excitation electron distribution as those of L1. The calculated electron energy levels of L1 and 2 are summarized in Table 2.

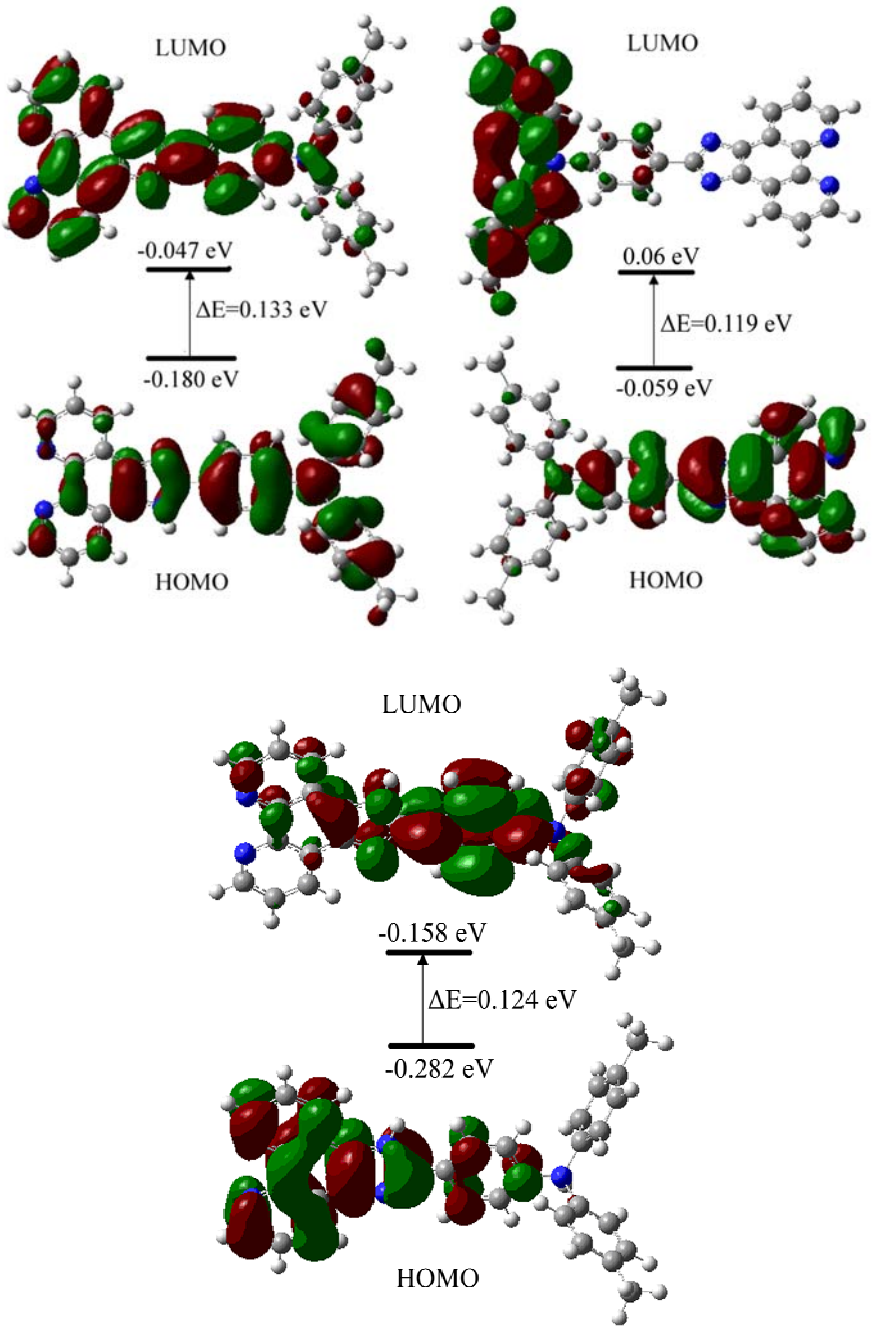


*Fig. 7. Electron distributions as well as HOMO and LUMO energy levels of L1, L1OH and L1H. (a): L1, (b): L1OH (deprotonated) , (c) : L1H (protonated)*

*Table 2 The calculated electron levels of L1 and 2.*

| Compds | L1 | L1O | L1H | L2 | L2O | L2H |
|---|---|---|---|---|---|---|
| HOMO(e | -0.18 | -0.05 | -0.28 | -0.18 | -0.05 | -0.28 |
| LUMO(e | -0.04 | 0.06 | -0.15 | -0.04 | 0.05 | -0.16 |

## 4. Conclusions

To conclude, we have designed and synthesized a new dye: 2-((4'-di(4-methylphenyl)-aminophenyl)imidazo[4,5-f][1,10]-phenanthroline (L1). Meanwhile, one similar derivative which has been reported previously has also been studied for the sake of comparison. Both compounds exhibited remarkably solvatochromic and solvatofluorchromic characteristics depending on the polarity of solvents.

Particularly, an acid/base induced absorption and fluorescent molecular switch has been demonstrated by modulating the ICT process from phenylamine group to the IP group via protonation/deprotonation. Besides, their The TPEF spectra were measured and their TPA cross-sections were obtained as 310 and 392 GM respectively. Meanwhile, charge-transfer (CT) states of both compounds were calculated through theory methods, which were well consistent with the results of the fluorescence emission changes observed during the experiments. The synthesis and property studying of L1 and 2 in this paper provide a model for researching these kind compounds as proton-induced OPEF and TPEF probes.

**Acknowledgments**

The authors greatly acknowledge the financial support of the State National Natural Science Foundation of China (No. 11104162 and No. 31100434),Talented Scientist of Shandong Province (BS2011CL035), and Science Foundation for colleges and universities in Jinan (201102052).

## References

[1] B. L. Feringa, Molecular Switches, Wiley-VCH, Weinheim, Germany, 2001.
[2] L. Z. Chen, G. Wang, X. C. Zhao, J. Lumin. **131**(8), 1617 (2011).
[3] S. Singh, B. D. Gupta, Sensor Actuat B-Chem **173**, 268 (2012).
[4] F. J. Wolter, S. H. Tessel, D. B. Otto, C. G. Ferdinand, J. Org. Chem. **75**(7), 2169 (2010).
[5] F. X. Cheng, N. Tang, J. S. Chen, F. Wang, L. H. Chen, Inorg. Chem. Commun. **14**(6), 852 (2011).
[6] Q. J. Ma, H. P. Li, F. Yang, J. Zhang, X. F. Wu, Y. Bai, X. F. Li, Sensor Actuat B-Chem **166–167**, 68 (2012).
[7] Y. Xiao, M. Y. Fu, X. H. Qian, J. N. Cui, Tetra. Lett. **46**, 6289 (2005).
[8] A. Coskun, E. Deniz, E. U. Akkaya, Org. Lett. **7**, 5187 (2005).
[9] D. Margulies, G. Melman, C. E. Felder, R. Arad-Yellin, A. Shanzer, J. Am. Chem. Soc. **126**, 15400 (2004).
[10] P. Passaniti, P. Ceroni, V. Balzani, O. Lukin, A. Yoneva, F. Vögtle, Chem. Eur. J. **12**, 5685 (2006).
[11] Z. X. Wang, G. R. Zheng, P. Lu, Org. Lett. **5**, 3669 (2005).
[12] S. Wang, S. H. Kim, Spectrochimica Acta Part A **72**, 677 (2009).
[13] S. H. Fan, K. Z. Wang, W. C. Yang, Eur. J. Inorg. Chem. 508 (2009).
[14] G. Y. Bai, K. Z. Wang, Z. M. Duan, L. H. Gao, J. Inorg. Biochem. **98**, 1017(2004).
[15] F. R. Liu, K. Z. Wang, G. Y. Bai, Y. A. Zhang, L. H. Gao, Inorg. Chem. **43**, 1799 (2004).
[16] F. Gao, H. Chao, F. Zhou, B. Peng, L. N. Ji, Inorg. Chem. Commun. **10**, 170 (2007).
[17] S. Z. Xiao, T. Yi, Y. F. Zhou, Q. Zhao, F. Y. Li, C. H. Huang, Tetrahedron **62**, 10072 (2006).
[18] S. H. Fan, A. G. Zhang, C. C. Ju, L. H. Gao, K. Z. Wang, Inorg. Chem. **49**, 3752 (2010).
[19] Z. Q. Bian, K. Z. Wang, L. P. Jin, Polyhedron **21**, 313 (2002).
[20] M. Sun, H. Xin, K. Z. Wang, Y. A. Zhang, L. P. Jin, C. H. Huang, Chem. Commun. **6**, 702 (2003).
[21] J. N. Demas, G. A. Crosby, J. Phys. Chem. **75**, 991 (1971).
[22] C. Xu, W. W. Webb, J. Opt. Soc. Am. B. **13**(3), 481 (1996).
[23] C. Hiort, P. Lincoln, B. Norden, J. Am. Chem. Soc. **115**, 3448 (1993).
[24] P. Fromherz, J. Phys. Chem. **99**, 7188 (1995).
[25] U. Narang, C. F. Zhao, J. D. Bhawalkar, F. V. Bright, P. N. Prasad, J. Phys. Chem. **100**, 4521 (1996).
[26] M. A. Albota, C. Xu, W. W. Webb, Appl. Opt. **37**, 7352 (1998).
[27] H. G. Zhang, X. T. Tao, K. S. Chen, C. X. Yuan, M. H. Jiang, Synth. Met. **161**, 354 (2011).

**Supplementary:**

**S1:** The 300 MHz $^{1}$H NMR spectra of L1 in DMSO-d6

**S2:** The 300 MHz $^{13}$C NMR spectra of L1 in DMSO-d6

**S3:** The electrospray mass spectrum (ES-MS) of L1

**S4:** Elemental analysis spectra of L1

**S5:** The 300 MHz $^{1}$H NMR spectra of L1 in DMSO-d6+NaOH

**S6:** The 300 MHz $^{1}$H NMR spectra of L1 in DMSO-d6+HCl

**S7:** The 300 MHz $^{1}$H NMR spectra of L2 in DMSO-d6

*Corresponding authors: haiguangzhang2006@126.com